

# CargoNet: A Low-Cost MicroPower Sensor Node Exploiting Quasi-Passive Wakeup for Adaptive Asynchronous Monitoring of Exceptional Events

Mateusz Malinowski, Matthew Moskwa, Mark Feldmeier, Mathew Laibowitz, Joseph A. Paradiso  
MIT Media Lab  
Responsive Environments Group  
20 Ames Street  
Cambridge, MA, 02142, USA

{mattxmal, mmoskwa, gepetto, mat, joep}@media.mit.edu

## Abstract

This paper describes CargoNet, a system of low-cost, micropower active sensor tags that seeks to bridge the current gap between wireless sensor networks and radio-frequency identification (RFID). CargoNet was aimed at applications in environmental monitoring at the crate and case level for supply-chain management and asset security. Custom-designed circuits and sensors were utilized to minimize power consumption and cost in a practical prototype. The CargoNet nodes are capable of asynchronous multimodal wakeup on exceptional events at extremely low power (Quasi-Passive Wakeup) with adjustable thresholds that adapt to dynamic environments. Accordingly, CargoNet has been seen to monitor, log, and report conditions inside a typical shipping crate while consuming under 25 microwatts of average power. To demonstrate the feasibility of the prototype system, several tests and deployments were conducted in the laboratory and aboard various transport conveyances.

## Categories and Subject Descriptors

B.4 [Hardware]: Input/Output & Data Communication

## General Terms

Measurement

## Keywords

Active RFID, Micropower sensing, Power management

## 1 Introduction

Radio-frequency identification (RFID), as used in the transport and distribution of goods, is a monumental improvement over bar codes, the technology that previously drove automation in the field. Because bar codes require line-of-sight between interrogator and tagged object, human operators must align a tagged object to ensure a read. Radio-frequency electromagnetic radiation used by most RFID tags, however, propagates widely and permeates through

most nonconductive materials, allowing identification without human involvement. This in turn has led to faster loading and unloading of goods, by as much as 80% [12].

While a bar code is printed onto a surface and cannot be changed, RFID tags are electronic circuits that can change state—and the ID of the tagged item—based on external stimuli. Early work used chipless systems for encoding sensor information (e.g., in a resonant frequency), such as near-field magnetic tags for human-computer interfaces and tangible media interaction [23] or surface-acoustic tags for tire pressure monitoring [28]. Recent efforts have focused on the development of sensate, chip-based passive tags, that are capable, for example, of sensing high temperatures with fuses that melt above a particular threshold [41] or that can detect when objects are manipulated through tilt switches [26]. Passive, multi-bit reporting of variable environmental conditions, such as ambient light, has also been implemented [35], in an RF-powered platform that contains a low-power microcontroller to sample and encode the light level. This leads to more functionality: the former RFID tag has evolved into a form that resembles a wireless sensor node, and when augmented by a small battery, such platforms are able to maintain some level of operation away from a reader.

The potential applications of such a hybrid platform are not difficult to imagine. Multinational corporations and their logistics specialists have started experimenting with battery-supported, or *active*, RFID to provide better “visibility” into their supply chains. By collecting data about environmental conditions experienced by goods in transit, they hope to better manage risk and maintain flexibility: potentially damaged goods can be inspected before they reach their destination and reordered if necessary [39]. The technology can also help assign responsibility for damage when multiple carriers are involved in the transport. As companies increasingly rely on global trade, these two concerns are driving the development of active RFID solutions.

The United States Department of Homeland Security (DHS) has recently been another potent force in the development of active RFID. DHS directives mandating electronic filing of container manifests and promoting electronic seals (e-seals) on containers [3, 40] will have an effect as companies employ automated systems to reduce the costs associated with more stringent border inspections.

Permission to make digital or hard copies of all or part of this work for personal or classroom use is granted without fee provided that copies are not made or distributed for profit or commercial advantage and that copies bear this notice and the full citation on the first page. To copy otherwise, to republish, to post on servers or to redistribute to lists, requires prior specific permission and/or a fee.  
SenSys '07, November 6–9, 2007, Sydney, Australia.  
Copyright 2007 ACM 978-1-59593-638-7/07/0004...\$5.00

In response to DHS initiatives and the quest for greater visibility, numerous companies have proposed and released solutions. The products available can be divided into two main categories:

- Omnibus platforms with numerous sensors, which are large and expensive and therefore applicable only at the level of the container. Examples include Savi Technology's ST-676 [31].
- Less expensive but more specialized platforms, which can usually sense only one modality (for example temperature for cold-chain management) [34, 36]. Numerous other active RFID platforms perform no sensing, and are only used for tracking.

There is currently no multimodal active RFID platform that is sufficiently small and inexpensive to be practically used at the level of the box, pallet, or crate, rather than an entire shipping container.

The challenge was therefore to develop a multimodal platform that remains both small and inexpensive. Since the size of an active tag is largely determined by its battery capacity, decreasing size while preserving a multi-year battery life requires micropower operation. Thus the major design tradeoff became one between low power and low cost, while providing a general platform for shipment monitoring. As summarized in this paper and detailed in [17], these factors have inspired our research into asynchronous and adaptive micropower wakeup from multiple sensors and informed our exploration into the utility of very low-cost off-the-shelf sensors for supply-chain application.

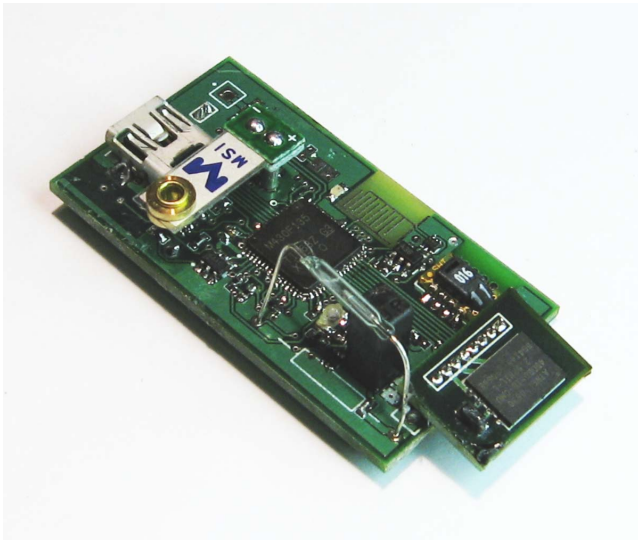


**Figure 1. A photograph of a CargoNet sensate tag, with external flash memory. A coin cell battery is accommodated on the underside of the unit.**

Achieving the above goals required the design and construction of a new platform—CargoNet. The platform (Figure 1) featured novel micropower sensors (with associated interface circuitry) and precipitated the development of an improved paradigm for micropower operation. This strategy, dubbed “quasi-passive wakeup”, uses the energy from the

stimulus to wake the microcontroller from its sleep state with dynamic thresholding. Energy is conserved by foregoing—where possible—polling and linear amplification, and the frequency of redundant wakeup is further reduced by desensitizing the sensors following repeating stimuli. Quasi-passive wakeup allows a cargonet tag to simultaneously and continuously monitor many sensor modalities for exceptional activity while dissipating minimal power.

The designs were constructed on a custom printed circuit board and tested first in the laboratory, then aboard a freight ship and cargo aircraft, and finally onboard a fleet of trucks. In the later tests, a CargoNet tag exploiting quasi-passive wakeup was compared against a co-located tag sampling continuously at 2 Hz. The CargoNet tag detected, processed, and logged the same stimuli (plus logged occasional abrupt events missed by the sampling tag), while maintaining an average power consumption of  $23.7 \mu\text{W}$ .

In the text that follows, Section 2 overviews the high-level CargoNet system, Section 3 details each of the CargoNet sensors and covers the particulars of the low-power and low-cost implementation of each one, Section 4 touches on a few features of the embedded code and system operation, and Section 5 presents results from several different tests of the CargoNet system, evaluating its low-power performance and introducing new efficient techniques for measuring extremely small supply currents in embedded sensor nodes. While suggestions for future improvements to CargoNet are distributed throughout this paper, our conclusions and recommendations for future work are summarized in Section 6.

## 2 System Architecture

A system diagram of the CargoNet tags and reader appears in Figure 2, and shows the MSP430 microcontroller, real-time-clock, and CC2500 2.4 GHz radio. These three components constitute the core of the system, and their choice contributes to the low power consumption and low cost of the system.

The well-known MSP430F135 flash-based microcontroller from Texas Instruments has a specified standby current of less than  $0.1 \mu\text{A}$  in its sleep state. This state offers RAM retention and startup from interrupt within  $6 \mu\text{s}$  [37].

The MSP430 series of microcontrollers is self-programmable. Its internal flash has a capacity of 16 kB, and any memory not dedicated to program storage can be used for data logging, further reducing system cost, complexity, and power consumption. Despite its small size it should suffice for routine use, as only extraordinary events (such as extremes of temperature and significant shocks) need to be recorded. Assuming the code consumes 8 kB, and potentially harmful or notable events occur once per day and require 10 bytes to log, the flash will last over two years before it is filled.

For testing purposes, and in cases where more detailed information is necessary, an external SPI flash memory can also be attached to the tag. Atmel's AT45DB081B, with 8 Mbit of capacity and a standby current consumption of  $2 \mu\text{A}$ , was used for most of our tests.

In addition to its fast-starting, high-frequency internal oscillator, the MSP430 can also use other clocks, such as a low-frequency watch crystal. Although this is the least

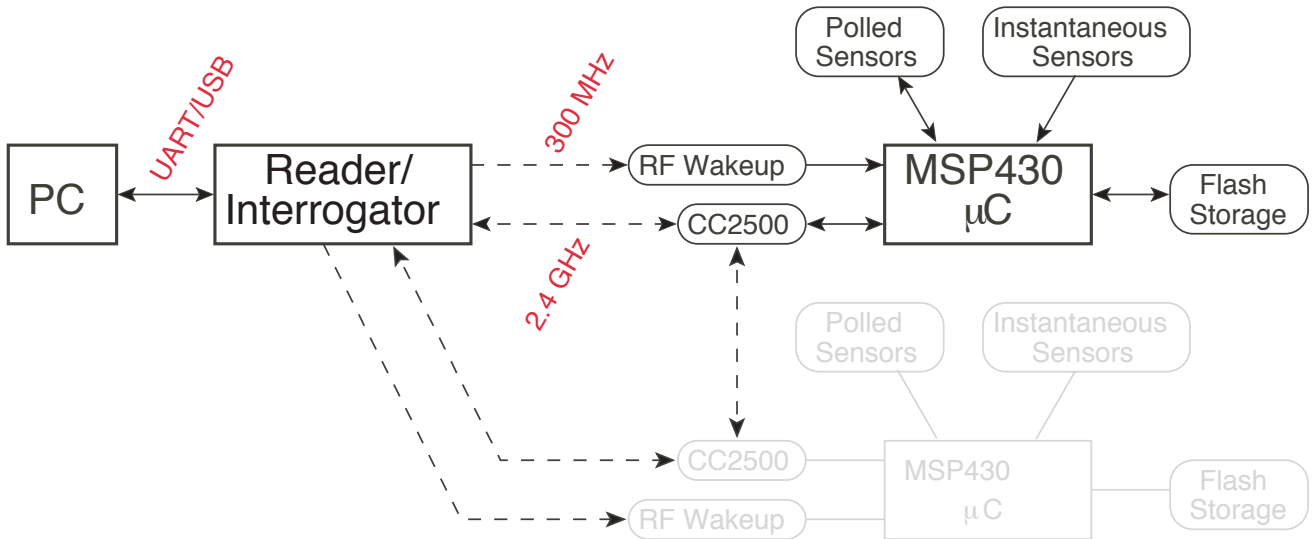


Figure 2. The CargoNet system with reader and additional tags.

expensive timekeeping solution, the MSP430 in this mode consumes  $1.6 \mu\text{A}$  [37]. By employing a separate Philips PCF8563 real-time clock (RTC) chip, this timekeeping current can be reduced to  $0.35 \mu\text{A}$  (the RTC itself consumes only  $0.25 \mu\text{A}$ ) [27].

Inferring that a shipment may have been damaged due to shock, tilt, or extremes of temperature and humidity can already be accomplished by using stick-on mechanical or chemical tags that change color when an exceptional event occurs. Additionally, some of the augmented passive RFID platforms mentioned in Section 1 can also communicate past state to a reader wirelessly. It is the presence of a RTC, however, that allows an active RFID tag to pinpoint *where* along the supply chain the damage occurred by measuring the time from the last checkpoint. The RTC also serves to initiate a once-per-minute polling sequence of the humidity and temperature sensors.

CargoNet tags use the CC2500 from Chipcon to communicate wirelessly with readers/interrogators. Because the radio is fully bidirectional, the tags can also receive instructions from the readers as well as communicate with each other. The latter is an ability that helps bridge the gap between active RFID and Wireless Sensor Networks (WSN), and enables useful applications, such as synchronizing clocks, recording the identity of neighbors, or qualifying the validity of sensor readings. As noted in Fig. 2, CargoNet nodes are also able to wake quasipassively upon receiving an RF amplitude burst at 300 MHz over a dynamically-adjustable threshold. This is exploited by a wireless basestation reader/interrogator that has been developed to query the tags for reports of significant events (e.g., temperatures or shocks over threshold), request data dumps, or adjust tag parameters [19]. A thorough discussion along with preliminary test results is presented in Section 5.3.

The system core and peripherals have been designed to be powered by a CR2032 lithium coin cell with a capacity of 235 mAh, but all testing has been performed so far with

an external 2-AAA alkaline battery pack to accommodate convenient development.

### 3 Sensor Hardware

The CargoNet tag achieves its low average power consumption by neither polling nor amplifying quickly-changing environmental stimuli. These are instead processed passively and compared against a threshold in a technique dubbed “quasi-passive wakeup”. The comparator used (Linear Technology LTC1540) is in essence an amplifier, but due to its nonlinear class-D operation, it typically consumes only  $840 \text{ nW}$  of quiescent power [14]. Of course, not all stimuli change quickly enough to warrant this technique, and some, such as temperature and humidity, are polled. A 12-bit accuracy polling sequence for one of the sensors, the Sensirion SHT11 temperature/humidity monitor, lasts only 55 ms, which when conducted once a minute corresponds to a duty cycle of 0.092% and an average power consumption of  $1.5 \mu\text{W}$ . This low-frequency polling does not dominate the power budget of the tag. In cases where a very fast response is required, quasi-passive wakeup on temperature might be accommodated via a PTC thermistor or other thermal sensor exhibiting a high impedance and sharp characteristic response.

The remaining two sensors, the RF wakeup receiver and “vibration dosimeter”, are anomalies in that they employ linear amplifiers to boost or integrate weak signals. The op-amps used, however, each consume only  $2.6 \mu\text{W}$  of quiescent power, a small price to pay for a valuable function such as asynchronous RF interrogation. The above sensors, which assemble a suite of measurements relevant to the transport of equipment and goods, are listed in Table 1 and described in detail in the sections that follow.

#### 3.1 Quasi-Passive Wakeup

“Quasi-passive wakeup” is a strategy of passively processing a signal, comparing the results against a threshold, and if the signal is strong enough to warrant interest, waking

Sensor Type	Measurement or Application
Shock Sensor	Potential impact damage
Vibration Dosimeter	Average low-level vibrations
Tilt Switch	Package orientation and shaking
Piezo Microphone	Events causing loud nearby sounds
Light Sensor	Container breach or box opening
Magnetic Switch	Package removed or box opened
Temperature Sensor	Overheating or potential spoilage
Humidity Sensor	Potential moisture damage
RF Wakeup	Query from reader or another tag

Table 1. List of sensors present on the CargoNet tag.

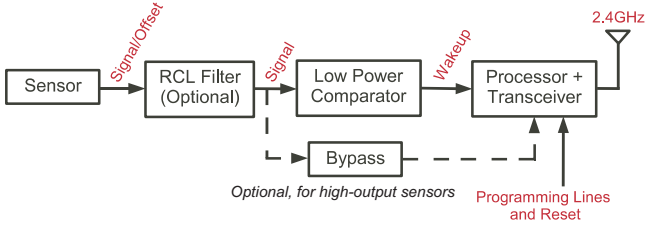


Figure 3. Block diagram of quasi-passive wakeup scheme used in the CargoNet system [24].

a larger system. A flow diagram is presented in Figure 3; this architecture is generalizable and has been used previously by our group in the FindIT Flashlight, a system of optically-interrogated ID tags [16, 2].

Although related systems have recently been explored elsewhere, they use significantly higher power with less sensor diversity. Researchers at Northwestern University have used a similar strategy for vibration detection and autonomous crack monitoring. Using a single geophone as the input sensor, their platform wakes up and records aperiodic shocks to ensure structural integrity of buildings. Although their analog front end consumes only  $16.5 \mu\text{W}$  on average, their processing is performed by a Mica2 mote, which adds a further  $105 \mu\text{W}$  to their average power budget [10]. Dutta and collaborators also mention detection of rare events with an interrupt-driven scheme, but because of their requirement-driven choice of sensors and their system design, they consume much higher power, e.g. several hundred microwatts or more [5]. The commercial T-Mote Invent platform comes with comparators to throw interrupts upon acoustic or acceleration stimuli, but the use of active accelerometers and microphone amplifiers pushes the needed power well into the mW range [1].

For quasi-passive wakeup to be practical, three things are necessary. First, the analog front-end, since it is always enabled, must consume on the order of a microwatt or less. In the case of millivolt signal levels, it will require a nanopower comparator such as the LTC1540 described earlier to boost the stimulus to logic levels and wake the microcontroller. Second, the active microcontroller core must wake up fast enough to adequately process the incoming stimulus. The MSP430, with a  $6 \mu\text{s}$  startup time is therefore ideal. Finally, the power consumption of the sensors and active components cannot dwarf that of the analog front-end (as in the geophone system) and duty cycles must be kept low by limiting the

number of wakeups and the amount of time spent in the active mode. The digipot that we use for adjustable wakeup thresholds consumes only 200 nA of quiescent current. The following paragraphs will discuss the micropower front ends, while the discussion of active-mode strategies will continue in Section 3.3.

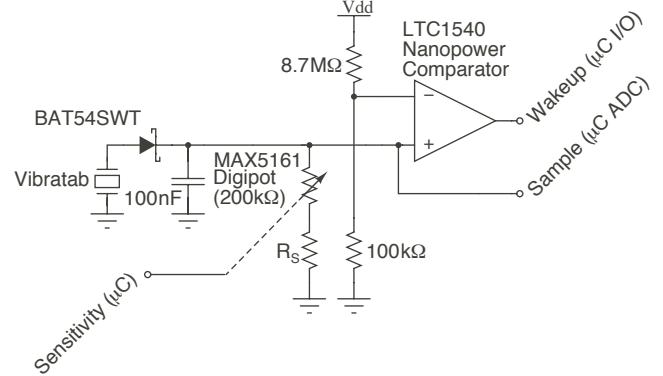


Figure 4. The digitally-controllable variable load resistor in the shock detector circuit effectively implements a dynamic threshold for shocks.

### 3.1.1 Shock Sensor

Most inertial measurement applications require an accelerometer to precisely measure shocks. Unfortunately, IC accelerometers are still relatively expensive and consume too much power to be ubiquitously used in everyday supply-chain applications, especially since the high resolution they provide is unnecessary when answering the question, “Did a shock occur?” Multi-axis sensing is also often superfluous, since the primary threat to the integrity of a shipment comes from drops, which cause sizable impulses that couple into all axes. Therefore, a passive one-axis shock sensor can be used, interfaced such that the energy from the shock alerts the microcontroller without any linear amplification.

The sensor used on our node is the LDTC MiniSense 100 (a.k.a. Vibratab) from Measurement Specialties. It consists of a cantilevered strip of flexible piezoelectric film encased in polyurethane, with a small proof mass at its tip; shocks set the mass in motion, and the piezoelectric film transduces the vibrations to voltage. Although the sensor’s resonant frequency is 75 Hz [18], we have found it to respond to vibrations up to approximately 1 kHz [17]. The Vibratab is very well suited to this application, as it produces a large (volts-level) open-circuit potential upon encountering even modest excitation. This property was exploited in one of the CargoNet’s predecessor devices, an ultra-low-cost, micropower, handheld wireless sensor that several of the authors had developed to enable interactive media control for a large audience [7].

As can be seen in Figure 4, the output of the vibratab passes through a peak detector. This strips the envelope from the high-frequency oscillations generated by the shock, reducing the sample-rate requirements that would otherwise have to be placed on the ADC to prevent aliasing when measuring the amplitude of the waveform. Neither the ADC nor the microcontroller is active when the shock first occurs;

instead, the filtered waveform is compared against a *fixed* threshold at the input of an LTC1540 nanopower comparator, the output of which wakes the microcontroller and starts the ADC sampling sequence via an I/O pin interrupt.

Although the actual threshold of the comparator is fixed at 40 mV, the sensitivity of the shock detector *can* be controlled. The peak detector is composed of a capacitor in parallel with a MAX5161 digitally controlled potentiometer (or digipot), which can be used to control the vibratab signal amplitude by varying the load resistance seen by the (high impedance) piezo sensor (the digipot could alternatively be configured here as a voltage divider, with its wiper feeding the ADC input). Comparing this variable signal to a fixed threshold, however, is equivalent to comparing a signal of a fixed amplitude to a variable threshold.

Such an arrangement is necessitated by limits on bias currents: the 40 mV threshold is set by resistors in the megaohm range, whereas micropower digipots are generally available up to 200 k $\Omega$ . The lack of dynamic range would make using the digipot to set the threshold directly impractical.

With the sensitivity of the shock detector thus dependent on commands from the microcontroller, the system can adjust its sensitivity. For example, the residual vibrations from a large jolt can persist for over a second. During this time, the microcontroller wakes up continuously and consumes power in vain, as no new information is imparted by these secondary stimuli. They are part of the same event and are of significantly less interest than the initial shock. Similarly, ships, trains, and trucks all vibrate, and if the noise threshold has been incorrectly set, the vibration sensor will continually wake the tag, eventually discharging its battery and preventing it from catching important events that may happen later. With the digipot in place, the noise threshold can be changed dynamically, depending on conditions.

### 3.1.2 Piezoelectric Microphone

A 2.5 cm-diameter piezoelectric microphone (Kobitone model 25LM015 [13]) has also been included in the platform - this transducer produces a strong electrical response to loud audio stimuli that can be indicative of nearby activity (e.g., something dropping, a metal door closing, etc.). Although the microphone is too large to be mounted onto the tag PCB, it can be easily connected to it via a pair of wires and situated nearby to pick up sudden sounds (Figure 5). The processing circuitry is similar to that for the vibratab presented in Figure 4, except for the absence of an envelope detector. Instead, the digipot loads the microphone directly.

Data collected by the microphone, as by the shock sensor and vibration dosimeter, also indicate sudden movement and impacts. The microphone responds to shocks that do not occur along the vibratab's primary axis of sensitivity, or shock events that produce acoustic frequencies. Furthermore, by analyzing the microphone waveform after wakeup (offline if samples are stored in flash or on the tag if the analysis is sufficiently simple), it may even be possible to determine what caused the impact, or whether an object inside the tagged shipment shattered. Perhaps most importantly, the microphone also detects phenomena causing loud acoustic events with no mechanical counterpart (e.g., nearby objects being struck or forced mechanical entry to the container).



**Figure 5.** A packaged prototype CargoNet tag used in tests, showing the piezoelectric microphone that can wake the microcontroller on loud sounds.

### 3.1.3 Switch Sensors

The CargoNet platform includes several binary sensors that indicate the presence of a potentially harmful condition. As with the vibratab and microphone, the sensors are neither polled nor permanently enabled—instead, they stay in a micropower state until the event occurs. In their activated state they consume non-negligible power (but still under 10  $\mu$ W), and once the condition has been logged or an alarm broadcast, the microcontroller can turn them off entirely. The sensors are then polled infrequently (currently every minute) to check for the continued presence of the condition; if it has been removed, the sensors are rearmed.

Two kinds of sensors are implemented to detect breach: a light detector/meter and a magnetic reed switch. Quasi-passive wakeup is simple to implement in the case of a light detector, as can be seen in Figure 6a. Essentially no current flows through the light-dependent resistor (LDR) in the absence of light, so if the circuit is powered, the output floats close to the positive supply. The load resistance (1 M $\Omega$ ) was selected such that the minimum amount of light necessary for an intruder to see in an otherwise dark room would bring the output of the circuit low and request a microcontroller interrupt. The LDR output is also connected to the on-chip ADC, which allows for the microcontroller to also quantify and log the intensity of light falling on the sensor when it is activated.

A dynamic threshold was not implemented in this circuit because the amount of illumination in a sealed box is assumed to approach zero, hence there is no “ambient” light level to which the circuit must adjust. If demanded by the application, however, a dynamic threshold could be easily added by inserting a digipot and nanopower comparator across the LDR, as in the shock and microphone sensors.

A magnetic switch provides another method to detect breach. The field from a permanent magnet placed on one

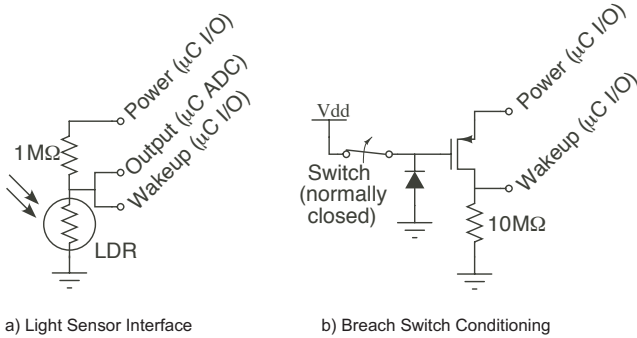


**Figure 6. Circuit schematics for LDR-based light sensor (a) and breach detector with magnetic reed switch (b), where the p-channel transistor conducts only when the switch opens, ensuring essentially zero current consumption under ordinary circumstances. These circuits can be enabled or disabled via output pins on the MSP 430, which maintain their logical states while the processor sleeps.**

of the flaps of a box or the lid of a crate holds the reeds of the switch together, closing the circuit. When the box or container is opened and the magnet moved, the reeds spring apart, opening the switch and waking the microcontroller, which logs the event and can broadcast an alarm. This sensor can also be used to detect the displacement of a package away from a docking position where a magnet is positioned to hold the switch closed.

Because the switch is normally closed, it cannot be optimally connected to the microcontroller like the LDR; a p-channel FET serves as a second, normally-open switch driven by the first magnetic switch. A reverse-biased diode connected to the gate conducts minimal reverse current when the switch is closed, but acts as a pulldown when the switch opens. The schematic for the circuit can be seen in Figure 6b.

Each tag also contains a tilt sensor, which is a one-axis ball-bearing switch (part number 107-1007 from Mountain Switch), mounted on the top layer of the PCB, such that the bearing rests on the electrodes when the tag faces up. This results in a switch that is closed under normal circumstances. A tilt of more than 90° starts the ball rolling down the shaft, opening the switch and alerting the microcontroller. The tilt switch accordingly responds to changes in package orientation or shaking. The behavior of this sensor is identical to that of the reed-switch breach sensor, so the circuit in Figure 6b was reused for this application.

### 3.2 Polled Sensors: Temperature & Humidity

Temperature and relative humidity (RH) are important parameters to monitor as they can vary widely over the course of a journey. The natural diurnal variations can be exacerbated by poorly insulated cargo holds on airplanes or leaky maritime containers, making monitoring a must.

#### 3.2.1 SHT11

The Sensirion SHT11 was used as the sole humidity and temperature sensor in the early versions of the CargoNet active tag. Unlike many of the offerings currently on the market, the SHT11 is not just a bare humidity sensor, but an integrated environmental monitoring subsystem that contains

temperature and humidity sensors, a 14-bit ADC, a serial communication interface, a ROM, and all drive and control circuitry. The SHT11 simplifies the task of the system designer (no need for separate drive circuitry or ADC) and also provides higher accuracy, as the unit comes factory-calibrated, with the calibration coefficients stored in the on-chip memory, a scheme that guarantees 3.5% accuracy between 20 and 80% RH, 0.03% RH resolution, and full interchangeability [33]. The SHT11 provides a calibrated reference against which to compare the inexpensive humidity and temperature sensors described below.

#### 3.2.2 Low-cost Humidity Sensor

Unfortunately, the SHT11 is by far the single most expensive component on the CargoNet, costing over USD 18 in quantities of 25 [20]. Less expensive humidity sensors tend to be no bargain either, since the cost of the necessary external drive circuitry consumes much of the savings. Resistive humidity sensors work by measuring the resistance across a hydrophilic polymer or ceramic; the low-cost Senser-HUM33 from Erlich Industrial Development Corporation, however, seems to use two interdigitated traces as the electrodes across the bare surface of a standard fiberglass-epoxy PCB [6]. By etching this design directly onto the PCB, it should be possible to achieve a simple humidity sensor (see Figure 7).

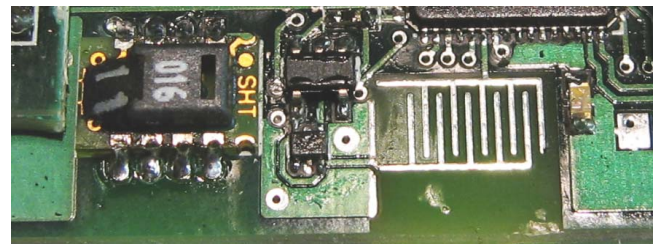


**Figure 7. Detail of a photograph of the CargoNet version 4 PCB shows the low-cost resistive humidity sensor (right) alongside the SHT11.**

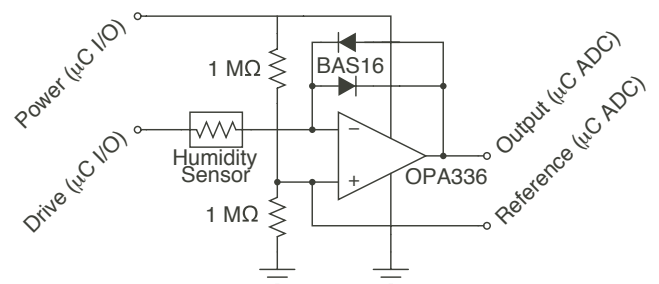


**Figure 8. Simple linearization circuit for low-cost humidity sensor.**

Resistive humidity sensors must be driven with an alternating signal with zero bias, as polarization may affect the sensor operation and differential sampling can compensate for drifting bias offsets. Furthermore, the resistance of the

sensor varies exponentially with relative humidity, and can range from less than 1 k $\Omega$  to well over 10 M $\Omega$  [29]. Figure 8 is a low cost (roughly 1.5 USD at 25-unit quantity) interface for this sensor, with low power assured through low-duty-cycle polled operation (a microcontroller I/O pin powers the amplifier and voltage divider). Once each minute, this power pin is asserted for 350 ms, during which the drive pin exhibits 3 cycles of a 3 V<sub>P-P</sub> square wave. Output values are sampled and subtracted at each polarity of the the last drive cycle, by which time the amplifier has stabilized. The feedback diodes produce a bidirectional logarithmic characteristic, which linearizes the sensor response. The peak-to-peak amplifier output voltage of this circuit decreases by approximately 100 mV for each decade of input resistance, and has been measured to work at well beyond 10 M $\Omega$  [17]. Although these sensors tend to decrease resistance exponentially with temperature [32], the diodes in Figure 8 exhibit their own temperature dependence (nominally  $-2\text{mV}/^\circ\text{C}$ ) that tends to cancel this effect: ideally the diodes should decrease the output voltage by 100 mV over 50  $^\circ\text{C}$  as the humidity sensor attempts to increase it by 100 mV. Since temperature is also directly measured on our board, it can be used to digitally compensate any remaining thermal effects in this humidity value.

### 3.2.3 Internal Temperature Sensor

The final revision of the CargoNet board contained two temperature sensors—the on-chip temperature monitor in the MSP430 and the calibrated temperature sensor in the SHT11. Provided that a low-cost humidity monitor such as described above could adequately work and the MSP430's temperature sensor can be easily calibrated, the SHT11 wouldn't be needed. Then temperature would come for free and humidity would come for only the cost of the components in Figure 8.

## 3.3 Micropower Active Sensors

Despite efforts to use quasi-passive wakeup and polled sensors throughout the tag, two active sensors had to be included on the tag, as signals from certain stimuli are too weak to be processed directly and must first be amplified. To minimize the power consumption from these sensors, micropower op-amps were used, namely the LPV511 from National Semiconductor and TLV2401 from Texas Instruments— both exhibit a quiescent power consumption of only 2.7  $\mu\text{W}$  and perform adequately for slow signals.

### 3.3.1 Vibration Dosimeter

The shock sensor described in Section 3.1, above, responds to and logs sudden, powerful vibrations, but lesser ones are ignored, as are—depending on the dynamic threshold—subsequent equally powerful vibrations that happen within a short time span after the initial hit. All these vibrations have an effect, and even though they will not damage the shipment through sheer impact, they may contribute to the loosening of screws and other mechanical connections. More generally, for shipment of certain sensitive goods, the net low-level vibrations encountered can have deleterious effects.

The so-called “vibration dosimeter” included in CargoNet consists of an active integrator built around a micropower op-amp, with low-leakage reset circuitry [9] and polyethylene

feedback capacitor, as can be seen in Figure 9. The microcontroller periodically samples and then resets the capacitor voltage to reduce the effects of leakage; additionally, the integrator is connected to a microcontroller I/O pin with interrupt capability, which is able to wake the microcontroller and request a reading/reset if the voltage suddenly climbs above the microcontroller logic threshold of approximately 1.5 V, as might happen upon a big impact or strong vibration.

The vibration dosimeter is connected to the same physical vibratab as the shock detector, but due to the reverse-connected Schottky diode at the input, it uses only the negative portion of the sensor's output signal, whereas the shock detector uses the positive. Because an active integrator inverts the input, the output will be positive and correspond to the integral of the encountered vibration peak.

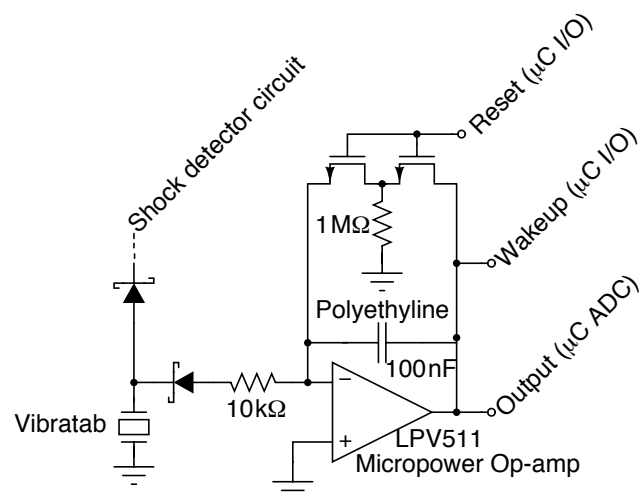


**Figure 9. The vibration dosimeter integrates the negative swings of the vibratab, keeping track of small vibrations.**

### 3.3.2 RF Detector

Like most of the commercial active tags described in Section 1, ours includes a secondary, lower-frequency, short-range signaling channel for interrogation and passing of location information in addition to the high-frequency, faster, longer-range radio for data communication with a reader. Because of the shorter range of the low-frequency link, the RF power delivered to the tag is high enough to wake it up; only then is the high-frequency radio—which consumes up to 20 mA of current in the case of the CC2500—powered on.

A 300 MHz, micropower detector has been implemented to detect interrogation from a reader. As can be seen from the schematic in Figure 10, the detector circuit consists of an LC tank with autotransformer, which doubles the amplitude of the signal voltage received at the antenna. This is followed by an envelope detector and a micropower amplifier with a digipot in the feedback attenuation for dynamic thresholding (a 50 k $\Omega$  MAX5161 selects gain factors between 20 and 1000, allowing sensitivity, hence spurious wakeups, to be decreased in noisy RF environments). The amplifier is biased near its midrail because its quiescent power consumption is minimized there. The envelope detector (or AM demodulator) consists of a forward-biased Schottky diode loaded by a

10 M $\Omega$  resistor, which also keeps the amplifier’s output normally below  $V_{cc}/2$  (at logic 0). The circuit presented here offers much more sensitivity than our prior design [17]. Other groups (e.g., [8]) have explored waking up sensor nodes with passive RF circuitry—the addition of a micropower amplifier offers more sensitivity with only minor power consumption.

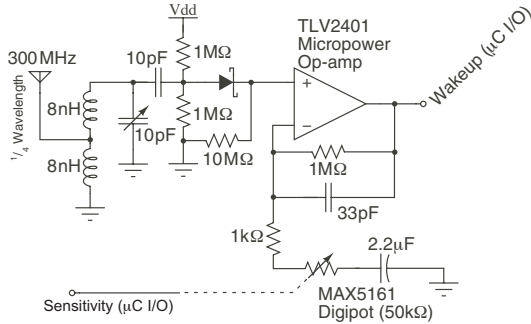


**Figure 10.** The RF detector circuit demodulates incoming 300 MHz radiation and boosts the signal across logic levels to wake the microcontroller.

### 3.4 Summary

The parts for the CargoNet platform with the above suite of sensors (minus the SHT11 humidity and temperature sensor, which was intended mainly for testing) cost around USD 40 in small quantities [17], which is admittedly far from negligible, but will decrease quickly with production quantity and may not be prohibitive when used in the transport of high-value items or at the pallet level. Of course, the platform is reusable, so the cost can be amortized over several years. The 10 gram CargoNet node of Figure 1 measures 64 x 26x 13 mm. Although smaller sensor nodes have certainly been made (e.g., [22], [25]) and node size will shrink even further (e.g., [21]), this device is already small enough for its purpose, and can easily be shrunk with an improved circuit layout (an appropriately-ruggedized version would also resin-pot the circuit board, leaving only sensors exposed as necessary). Costs have been limited by employing simple fabrication techniques, as well as inexpensive sensors and off-the-shelf parts.

The power budget in Table 2 shows the quiescent power consumption for each sensor module as designed. A CR2032 coin cell will last over 5 years at this level of quiescent drain, and the AAA batteries used in our tests scale out to over 25 years, which is of course well beyond their shelf life. This is only a rough indicator of actual system power consumption, since much will depend on the duty cycle of the sensors. The balance struck between active and quiescent states, controlled by the firmware, is elaborated further in the next section.

## 4 Embedded Software and Operation

Because of cost and power constraints, the CargoNet platform has at its core a Texas Instruments MSP430 16-bit processor with 512 bytes of RAM and 16kB of storage, which must control the sensors described in Section 3, process and store received data, and respond to readers and communicate with other tags nearby. Although the hardware has already been designed to maintain low power consumption in

its quiescent state, it rests on its custom-designed firmware (7.5 kB, custom-coded in C) to control the duty cycle and active-mode operation.

This mandates that the system be completely interrupt driven, with the processor switching to the next waiting task or retreating to one of the low-power modes whenever it is not being used. Since most of the sensors have already been designed to interrupt the microcontroller if an important event occurs, the structure of program execution is straightforward: wake up, process data, and return to sleep. The details of the embedded code are provided in [17], and a couple of particular procedures are described below.

### 4.1 Dynamic Thresholds

Dynamic thresholding was presented in Section 3.1 as a strategy for limiting the number of successive wakeups due to a single event. Each wakeup averted corresponds to power saved, as the tag remains in a sleep state for longer periods of time.

The simplest way to limit wakeups is with a blackout period following each one, during which interrupts from the sensor that caused the wakeup are disabled. Such a scheme would make the tag insensitive to all stimuli during the blackout period, even if the latter were more noteworthy than the first. It is possible, for example, that during a drop, a single corner of the monitored container would hit the ground before the rest. In this case the tag would ignore the main event, having woken up when the first corner hit the ground.

The strategy used in CargoNet is more nuanced: rather than switching a sensor off after a wakeup, the tag “numbs” it with a digitally controlled potentiometer. The tag begins operation with this digipot, a MAX5161, at the maximum resistance setting, to detect the smallest signal of interest. With each successful wakeup, the interrupt-handling routine for the sensor just stimulated decreases the resistance to load the sensor, thereby attenuating its output voltage (which is compared against a fixed reference).

The digipot resistance is decreased by a predetermined power of 2, in an approach reminiscent of exponential back-off in Ethernet and other communication protocols. The resistance is then successively increased whenever the tag wakes up each minute to poll temperature and humidity sensors. The sensor is thus gradually readied for new stimuli. The system is also amenable to more complex adaptation schemes: for example, the tags could vary the dynamic thresholds so as to maintain an average wakeup rate—and by extension power consumption—at some preset level, as has been done in other systems [15].

### 4.2 RF Synchronization

When a stimulus above the current threshold is detected by the tag, it wakes up and collects the data (if analog) using the on-chip ADC. It then processes the data (in the case of a shock waveform, only the maximum is currently saved) and logs it to memory for later analysis. If the shock is significant enough, an alarm is then sounded via the CC2500 2.4GHz radio to any readers that may be listening in the vicinity, as may be possible in a warehouse or the hold of a cargo ship.

In case there are no readers to receive the alarm, nearby tags can also receive and log it. Such an exchange of data between tags—something that is not currently implemented

Module	Component	Typ. Quiescent Current [ $\mu\text{A}$ ]
Microcontroller	MSP430F135 Microcontroller	0.1
Radio Transceiver	CC2500 RF Transceiver IC	0.4
Real-Time Clock	PCF8563 Real-Time Clock IC	0.25
Low-Cost Humidity Sensor	(OPA336 + Resistor Divider)*0.35/60	0.1
Light Sensor	Standard LDR	0.1
Reed Switch	NTJD2152 FET	0.01
	BAS16DXV Diode	0.004
Tilt Switch	NTJD2152 FET	0.01
	BAS16DXV Diode	0.004
Shock Sensor	LTC1540 Comparator	0.3
	MAX5161 Digipot	0.2
	Resistor Divider	0.36
Vibration Dosimeter	LPV511 Op-amp	0.9
	2N7002DW FET	0.025
RF Detector	TLV2401 Op-amp	0.9
	MAX5161 Digipot	0.2
	Resistor Divider	0.5
Piezoelectric Microphone	LTC1540 Comparator	0.3
	MAX5161 Digipot	0.2
	Resistor Divider	0.5
Total Current at 3V		5.36

**Table 2. The quiescent power budget for the CargoNet active tag, based on manufacturers' typical figures.**

in commercial tagging platforms—would be beneficial for a number of reasons. First, in the absence of reliable references, synchronization between tags is a good way of keeping the real-time clocks from drifting. A tag can adjust its clock by averaging received time stamps and comparing the result with its own time stamp for the event. Synchronization would also enable tags to keep track of their neighbors, a concern in the transport of hazardous cargoes, where certain materials must be kept strictly apart. Furthermore, inspections could be streamlined, as only one tag would need to be read to ascertain the state of those in the vicinity. A fourth potential application of RF synchronization would be to verify the validity of sensor readings through comparison with neighbors, and to keep duplicate records of events in case the tag itself were to undergo damage. Such synchronization could be instigated by diverse stimuli—e.g., via the acoustic channel with a very loud sound waking all the tags within its reach. A deliberate synchronization command could also be transmit, for example via the 300 MHz wakeup channel or via structured acoustic pulses (as the audio signal is digitized, the processor can analyze it for an FSK code once it is awoken).

## 5 Testing and Analysis

Several tests of the CargoNet platform were performed, both in the laboratory and in the field, to verify the performance of the hardware and firmware designs. Further tests would be necessary to calibrate the on-board sensors, and to guarantee operation of the platform under the conditions experienced by intermodal cargo. The results presented in this section, however, demonstrate that CargoNet has met its design goals of providing micropower environmental sensing in a small and inexpensive package. More testing details than can be summarized here are available in [17].

### 5.1 Singapore to Taiwan

The CargoNet tags were briefly tested in the laboratory and in a container yard, where they were subjected to the shocks common in the moving and stacking of containers. Soon afterwards, seven CargoNet active tags were augmented with an external 8Mbit flash memory, external piezo microphone, and two AAA alkaline batteries, placed inside small ABS plastic cases for safety (Figure 5), and sent to Singapore as part of Intel Corporation's tests of their Intelligent Container Project. Upon arrival in Singapore, they were placed on the floor of an empty shipping container and proceeded to record the conditions inside the container. The container was loaded onto a cargo ship and traveled for a week between Singapore and Kaohsiung, Taiwan, and the tags continued to record for up to three additional weeks as they made their way back to the United States for analysis (a firmware bug resolved on our subsequent tests increased the average power consumption, resulting in truncated tag lifetimes for the Singapore run).

#### 5.1.1 Tilt Switch

The tilt switches on board the tags performed without failure during the Singapore test, though they tended to be overly sensitive. As can be seen in Figure 11a, the switches could open shortly after being re-armed by the microcontroller during the active part of the polling cycle. This indicates that the sensor was responding not just to tilt but to sudden shocks that bounced the ball bearing inside the switch up from the contacts, breaking the circuit.

#### 5.1.2 Vibration Dosimeter

Figure 11b shows the raw dosimeter data, as collected by the ADC once per minute or more. One can clearly see spikes at times when large shocks occurred, which correspond to the tilt-switch records in Figure 11a.

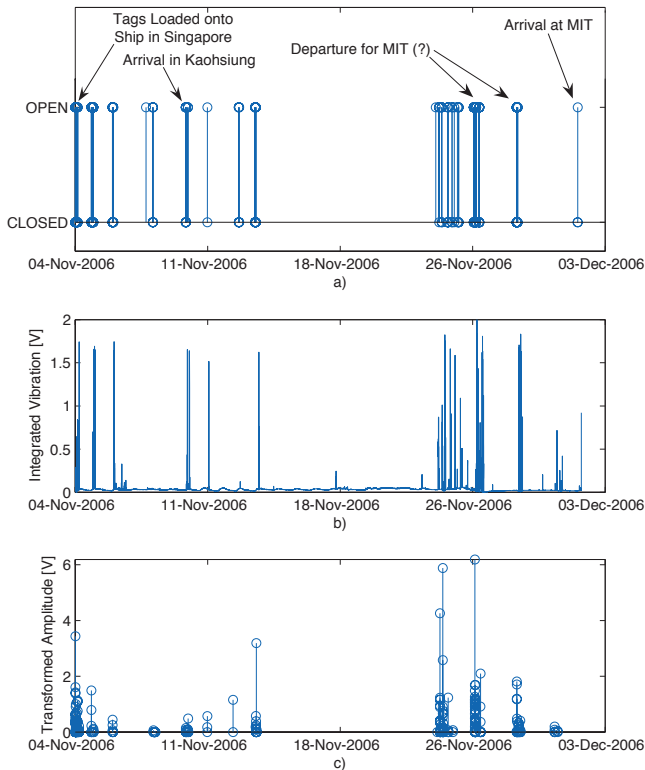


**Figure 11. Comparison of the responses of the a) tilt switch, b) vibration dosimeter, and c) piezoelectric microphone (circles denote a wakeup).**

Looking closer at Figure 11b, it becomes clear that the small vibrations at the lower range of the scale exhibit diurnal cycles. These variations are proportional to temperature, and were most likely caused by temperature-dependent offset voltages in the integrator op-amp; these offsets (which will vary between tags) can be corrected by subtracting a temperature-dependent offset from the waveform during analysis, and eventually on board the tag during data collection. A more precise op-amp in the integrator could also lessen the magnitude of this error, albeit with added expense.

### 5.1.3 Piezoelectric Microphone

The piezoelectric microphone was the only sensor that used dynamic thresholds during this test (the vibratab shock sensor worked too sporadically due to high thresholds, and the RF detector part of the tag was not implemented), and it worked surprisingly well at picking up acoustic counterparts to the large mechanical excitation that also tripped the tilt switch and peaked the vibration dosimeter as seen in Figure 11c.

In general, Figure 11 compares the responses of three different sensors. Although they all seem to trigger with any large shocks experienced by the tag, there is considerable diversity to how they respond to the events. Properly capturing all aspects of the tag's mechanical environment therefore benefits from a multimodal sensor suite.

The effectiveness of the dynamic threshold mechanism is more difficult to evaluate, as there were no tags without dynamic thresholds implemented during this test to serve as a

control group. The tags logged decreasing sensitivity with each successive wakeup, but large shocks would still wake the microcontroller at the lowest sensitivity level.

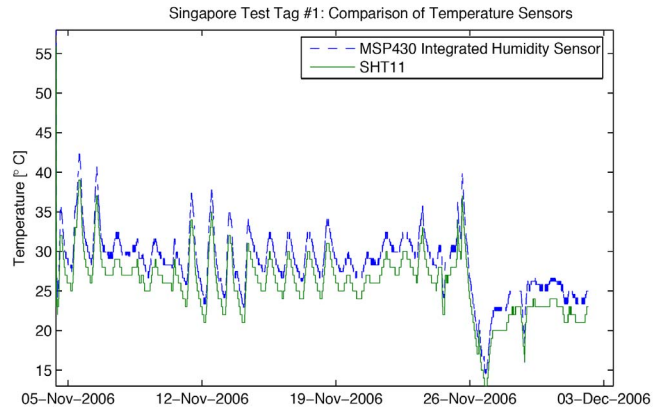


**Figure 12. Data from both onboard temperature sensors for the Singapore Test**

### 5.1.4 Temperature Sensors

Regarding the performance of temperature sensors, it is important to note the wide range of offsets produced by the MSP430's internal temperature sensor. Although the free internal temperature sensor has a maximum resolution of  $0.1^{\circ}\text{C}$  [37, 38], the accuracy of the sensor is not well specified. During the Singapore test, however, the readings of the sensor stayed within  $\pm 1^{\circ}\text{C}$  of the expensive, factory calibrated SHT11, despite a significant offset. This is seen in Figure 12, which shows temperature readings from both sensors diurnally cycling throughout the duration of the Singapore deployment. The MSP430 datasheet specifies a maximum offset error of  $13.7^{\circ}\text{C}$ , and offsets as large as  $12^{\circ}\text{C}$  were observed. These offset errors can, however, be easily eliminated with a simple calibration performed during the initial programming of the tag. Lab tests indicate that the operation of the MSP430 core at these very short duty cycles should have little effect on its temperature sensor—in ambient room conditions, the temperature reading was seen to climb by less than a degree after the processor was continuously running for a full minute.

## 5.2 DHL Express Air Test

To resolve some of the questions left unanswered during the Singapore test, several CargoNet tags were packaged and sent across the United States, from Cambridge, MA to San Francisco, CA, via DHL's overnight service. One of the tags was augmented with an external current measuring circuit similar to Jiang, et al's [11]. Like Jiang's circuit, it produces a series of pulses which are proportional to the current consumption, in this case each pulse represents 1nA sourced from a 3.3V supply.

But, instead of using a current sense resistor, differential amplifier, and voltage to frequency converter, all of which are very susceptible to temperature drift and cause droop on the power supply with increased current draw, the circuit implemented here uses a crystal oscillator and a current source to meter out precise amounts of current. A feedback circuit then maintains the output voltage at the required level

by adding more current pulses to a smoothing capacitor. The circuit obtains less than 1% variation in linearity over a range of .03 $\mu$ A to 3mA. The inaccuracies at low current levels are due to leakage in the smoothing capacitors, and at high currents due to base drive current in the current mirror. The feedback circuit keeps the ripple voltage on the power supply to less than 20mV for frequencies above 100Hz. At lower frequencies, high current draws (in excess of the circuit's capacity) cause droop due to the finite output impedance of the current supply.

This method of power metering could also be accomplished through an inductor, rather than a transistor current source, reducing the power loss of the metering power supply. In effect, this would be the same implementation as a switching power supply (buck or boost) where the switch on/off time is determined by the current through the switch (a common topology that is commercially available). A simple counting of the number of on/off cycles would then give an accurate measure of the current consumed, limited by the variation in the inductance due to temperature and humidity. We are now developing this single-unit power supply, which would essentially give current data for no extra power consumption or parts count.

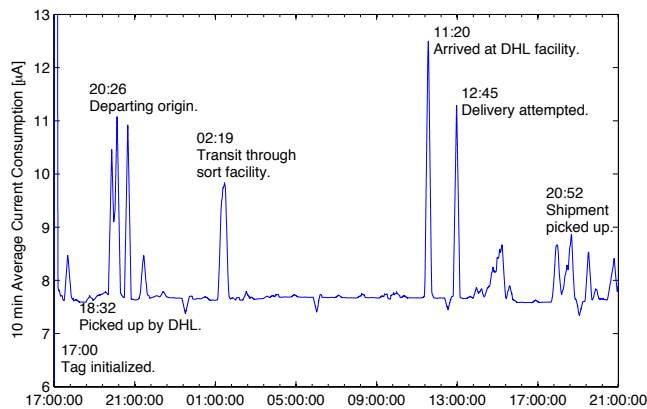


**Figure 13. Average current consumption of a CargoNet tag during an overnight journey from Cambridge, Mass. to San Francisco, Calif. Periods of higher current clearly correspond to episodes in its history during which it was handled or loaded from one conveyance to another [4].**

Along with this tag, which was having its current monitored under normal operation, the same box housed a second tag, which acted as a control and logged all sensor data at regular intervals of 500ms. This record can then be used to confirm the ability of the quasi-passive wakeup and dynamic threshold mechanisms to catch transient phenomena with sufficient resolution while saving power.

The current consumed by the monitored tag, averaged over a 10-minute window, can be seen in Figure 13. The current consumption increases whenever the shipment is transferred, and the shocks wake the tag. Notwithstanding, the average current consumed during the overnight journey to San Francisco was 7.88 $\mu$ A, which at 3V corresponds to an

average power consumption of 23.7 $\mu$ W. Accordingly, the tags arrived without any detectable depletion of their batteries. This amount is slightly more than the predicted current consumption of 5.36 $\mu$ A listed in Table 2, but the discrepancy narrows when taking into account the external flash added for the tests. Further statistics are presented in Table 3.

	Current [ $\mu$ A]	Power [ $\mu$ W]
Average	7.88	23.7
Maximum	556	1670
Standard Dev.	28.3	85.2

**Table 3. Current and power consumption of CargoNet during DHL test. All statistics calculated from data sampled at 500 ms.**

Figures 14 and 15 show the efficacy of using quasi-passive wakeup with dynamic thresholds versus periodic sampling when logging sudden shocks and sounds. As can be seen in the figures, the quasi-passive wakeup scheme is able to capture the same events with often a better level of detail than the periodic sampling method, while consuming orders of magnitude less power. In all fairness, the 2Hz sampling frequency was chosen based on the available storage capacity, and is often too slow to capture the events of interest. A more intelligent scheme, which samples at a higher frequency but logs only meaningful samples, could capture more data but would require even more power. As the microphones were enclosed in a shipping box, which muffled external sounds, their sensitivity was lowered. Accordingly, some low-level acoustic stimuli, encountered later in the test, didn't register a wakeup. If desired, acoustic sensitivity can be increased at minimal additional power cost by using a micropower amplifier as described in Section 3.3 (as these devices tend to be slow, large gain factors would favor lower frequencies).

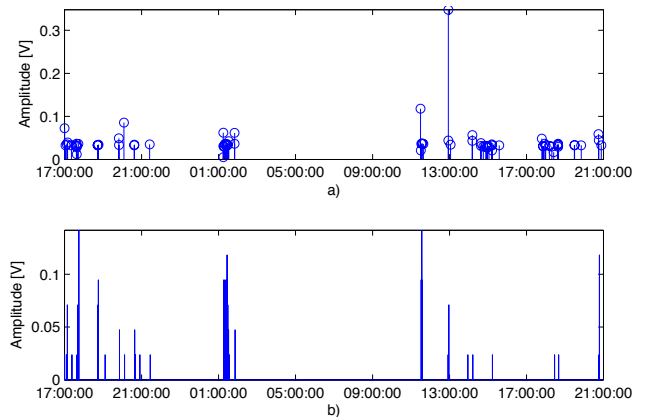


**Figure 14. Comparison of vibratab shock sensor readings collected with quasi-passive wakeup with dynamic thresholds (a) to those collected by sampling the sensor every 500 ms (b).**

### 5.3 Laboratory Tests

The tests between Singapore and Taiwan demonstrated the correct micropower operation of the the quasi-passive

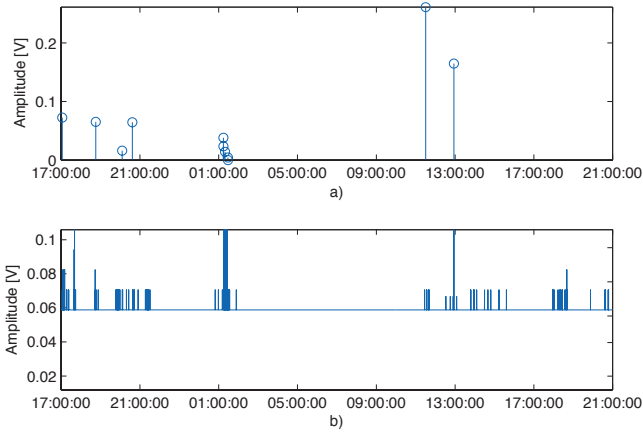


**Figure 15. Comparison of piezoelectric microphone readings collected with quasi-passive wakeup with dynamic thresholds (a) to those collected by sampling the microphone every 500 ms (b).**

shock detector, piezo microphone, and tilt sensors, as well as the polled temperature sensor. The remaining sensors were evaluated in the laboratory.

### 5.3.1 Light Sensor Test

The tests of the CargoNet node detailed above used a surface-mount phototransistor as a light sensor [17], which exhibited limited sensitivity, and couldn't reliably detect light leaked from a container or package breach. As indicated in Figure 6, the present circuit uses a common small (5mm) LDR—with the 1 M $\Omega$  series resistor, the sensor voltage drops below the logic threshold of the microcontroller's input at very low light levels, indeed triggering an interrupt whenever enough light to see was present, then going into once-per-minute polling mode until the light levels again dropped. When the circuit was active, the 1 M $\Omega$  series resistor kept the current consumption well below 1  $\mu$ A without preventing satisfactory ADC sampling of light levels.

Figure 16 shows data from all CargoNet sensors (except the low-cost humidity sensor) in varied environments across 24 hours of a hot August day in Cambridge, MA. This figure includes data from the light sensor—as it was extremely sensitive, we covered it with a perforated piece of electrical tape to keep the daylight readings from saturating. One can see that the light sensor software switched from polled to interrupt mode once the node was brought into a dark courtyard at around 10 PM and (excepting for a brief burst of light shortly after midnight) it stayed dormant until sufficient dawn light was encountered shortly before 6 AM (without the tape, it would have woken much earlier). The other sensors are seen to respond as noted in Section 5, with the tilt switch responding to node orientation and movement as the node is handled or transported, and the shock, dosimeter, and microphone signals responding mainly when the node was being hand carried. As the environments where this node was left weren't very noisy, most microphone signals look to be associated with the tag being jostled as it is moved. No battery degradation is noted across this test, certainly as expected with the low current drain demonstrated in Section 5.2 and

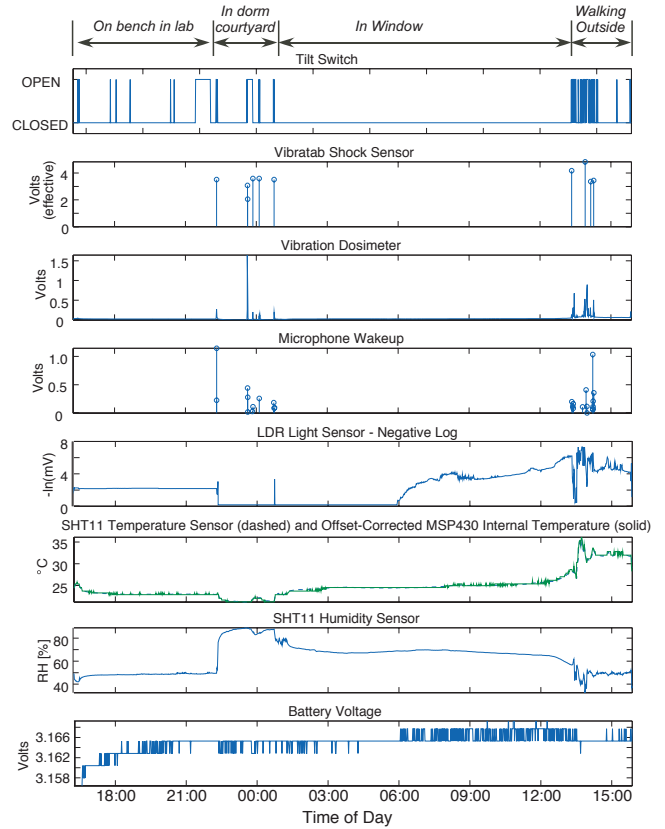


**Figure 16. Multimodal data from a CargoNet node taken across a full August day**

the dual AAA source (the positive transition at the beginning is due to the batteries recovering after being shorted before the microcontroller was reset).

### 5.3.2 Low-Cost Humidity Sensor Test

The low cost humidity sensor composed of interdigitated traces on the CargoNet PCB was not calibrated properly in our field tests. First, a firmware bug corrupted the SHT11 humidity readings during the Singapore test, preventing a proper comparison. Then, during the DHL test, the cold winter air inside the package kept the relative humidity below 20%, too low to register on the low-cost sensor. As a result, the humidity sensor had to be tested in the laboratory, using the on-board, calibrated SHT11 humidity sensor with 2% RH accuracy as a reference. Despite Erlich's stated 2.7% accuracy between 3 and 97% RH [6] for their seemingly similar sensor, tests of our circuit in an environmental chamber proved considerably less reliable, with no useful response below a RH of 60%, although above this value the low-cost sensor reading tended to vary quadratically with the SHT11's humidity measurements [17].

To attain better performance at minimal cost, we have recently explored an innovative approach proposed in [30], which creates a very cheap resistive humidity sensor by cutting the top off of a capacitor, thereby exposing its dense insulator-plate spacing to open air. This device (made from a standard 5.6 nF ceramic disc capacitor) exhibited considerable sensitivity, showing strong response to moisture in

breath, for example. Testing and evaluation are still underway. Although accuracy and repeatability of such a sensor may indeed be issues, this approach promises to provide a coarse estimation of ambient humidity, which may be sufficient for many supply chain applications.

### 5.3.3 RF Wakeup Test

The CargoNet tag as tested thus far did not include either the RF detector/wakeup circuit or the CC2500 2.4 GHz radio, as the focus has been on demonstrating the feasibility of micropower environmental sensing. In general operation, data must be collected off the tags at some point, however, so radio interrogation and communication are crucial.

The RF wakeup circuit described in Section 3.3.2 has been built and tested at 300 MHz, with the interrogation signal a 25 Hz square wave. Initial tests with a quarter-wave whip antenna attached to the board have demonstrated successful detection of signals above -65 dBm while consuming only  $2.8 \mu\text{W}$  of power. At maximum sensitivity, this circuit was able to reliably detect an OOK (On-Off-Keying) signal from a 3 Volt key fob transmitter (based around the Ming TX-99) located 8 meters away. To insure reliable and sensitive detection at minimal increase in power and cost, the amplifier output of Figure 10 should be discriminated by a nanowatt comparator, such as introduced in 3.1. Although the circuit shown in Figure 10 is able to adjust its sensitivity, we have not yet tested the performance of adapting wakeup thresholds to the ambient RF environment, and this remains a topic for future work.

Following interrogation, the CC2500 2.4 GHz radio is enabled, and successful communication and bidirectional exchange of data with a custom-built reader [19] have also been achieved. Design refinement exploiting established RFID technology promises to significantly improve the performance of this circuit.

### 5.3.4 Dynamic Threshold Test

The DHL overnight test indicated that a sensing platform built around quasi-passive wakeup is capable of detecting the same events as a tag with periodic polling, while consuming a fraction of the power. But what about the use of dynamic thresholds? That decreasing the sensitivity of the sensors would limit the number of wakeups to the repeated stimuli or residual vibrations seems obvious, but the efficacy of the dynamic threshold scheme present in CargoNet was put to the test in the laboratory.

A simple experiment was devised using a pair of identical CargoNet tags mounted onto a wooden plate and dropped onto a table at varying heights. Although both tags used the same initial detection threshold on the Vibratab shock sensor, one of the tags (Tag 2) ran the dynamic threshold scheme described in Section 4.1, while the other tag (Tag 1) kept its threshold constant. Fig. 17 shows the number of wakeups encountered by each tag as the drop height increased and the plate bounced around on the table. A linear increase in the average number of triggers (over 10 tests run at each height) can be seen for the statically discriminated Tag 2, while the dynamic discriminator on Tag 1 consistently produced only one trigger, except at the largest height, where the secondary shocks were big enough to very occasionally trigger another wakeup, indicating that the dynamic threshold is effectively adapting the tag against consistent stimuli.

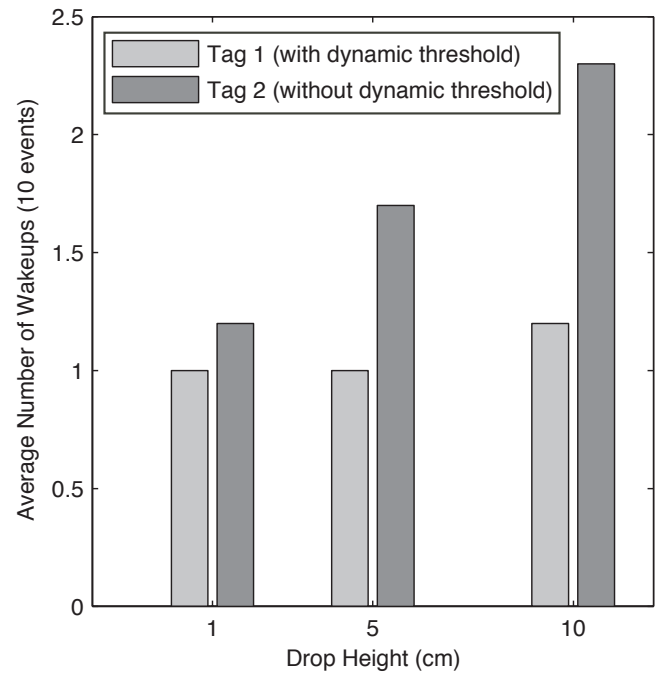


**Figure 17. Number of wakeup triggers resulting from static and dynamic thresholds for tags dropped at different heights**

### 5.3.5 RF Synchronization Test

As was mentioned in Section 4.2, the tags are able to use their on-board 2.4 GHz radios to synchronize—exchange data following an exceptional shared stimulus, such as a large shock (in order to minimize radio current consumption, this type of event should be chosen to be somewhat rare). This procedure would allow for the synchronization of clocks as well as the identification of and logging of neighbors for later analysis.

The RF Synchronization mechanism has been tested in the laboratory. Two tags were dropped simultaneously, and then were allowed to exchange information about the incident: a time stamp, source tag ID, the type of stimulus (in this case, shock), and its magnitude. The tags employed a simple carrier-sense/exponential-backoff protocol to avoid collisions. Following the shock, each tag switches its CC2500 to receive mode and then listens for a random period of time. After this interval has expired, the tag firmware checks for carrier (implemented using the carrier-sense feature of the CC2500), and provided the channel is clear, it begins to transmit data pertaining to the event, then returns again to listening until the maximum time allocated for all tags to transmit has expired. If another tag has already begun to transmit and a carrier is detected, the tag doubles its listening interval and returns to receiving. Although our tests of this protocol have been limited, it has worked well in the laboratory, and this scheme promises to be effective at exchanging multiple packets between tags following a collectively-noticed exceptional stimulus.

As the RF wakeup circuit described in Sections 3.3.2 and 5.3.3 has been demonstrated to be sensitive to mW-level

transmissions from small, easily integrated radios, it could be possible for proximate CargoNet tags to wake one another up via RF when one tag encounters an exceptional event worth reporting that doesn't necessarily contain a common environmental sensor stimulus. As stated in [8], direct RF wakeup promises energy savings of 70-98% (depending on the protocol used) over standard polled RF listening approaches.

## 6 Conclusion

The work described in this paper fills an important niche in the current efforts to add visibility to the supply chain. Through the development of quasi-passive wakeup and dynamic thresholding and a full suite of novel environmental sensors, the authors have developed and demonstrated a low-cost and extremely low-power platform that effectively bridges the gap between active RFID and wireless sensor networks. The resultant CargoNet tag, which was tested in the laboratory and aboard cargo ships, delivery trucks, and express courier aircraft, has demonstrated under  $25\mu\text{W}$  of average power consumption while keeping a full suite of detection sensors continuously alive—to the authors' knowledge, no other embedded sensor platform exhibits adaptive multimodal detection at such a low quiescent power. The asynchronous detection capability of the CargoNet tag has been shown to be commensurate with that of a frequently-polled platform, and although more sophisticated adaptation schemes can be employed, the CargoNet was seen to effectively exploit its dynamic thresholding capability to avoid multiple wakeups on correlated stimuli. While our CargoNet tests were shown to promise agile detection at low power with very low-cost sensors, a next step is to take a ruggedized array of CargoNet platforms into realistic but controlled environments for establishing optimal sensor and threshold calibrations together with the associated event classification algorithms needed for relevant supply-chain monitoring scenarios. Although more work remains on identifying optimal communication protocols for this device, the performance of adaptive communication features, such as stimuli-driven RF synchronization and passive RF wakeup, have also been explored and demonstrated.

## 7 Acknowledgments

The authors would like to extend their thanks to PepsiCo and the Things That Think consortium for funding this research, and to Mary Murphy-Hoye of Intel and Julius Akinyemi of PepsiCo for providing the initial inspiration for CargoNet, supporting our field tests, and for their sustained excitement and suggestions throughout the course of the project. Additional thanks go to Intel's Intelligent Container project team and other members of the Responsive Environments Group at the MIT Media Lab who helped with this project (Rachel Bainbridge, in particular, is acknowledged for running our final humidity and data logging tests).

## 8 References

- [1] Tmote invent user's manual. Technical report, Moteiv, Inc., San Francisco, California, February 2006.
- [2] G. Barroeta Perez, M. Malinowski, and J. A. Paradiso. An ultra-low power, optically-interrogated smart tagging and identification system. In *Fourth IEEE Workshop on Automatic Identification Advanced Technologies (AutoID2005)*, pages 187–192, Buffalo, NY, Oct. 2005.
- [3] Department of Homeland Security: Bureau of Customs and Border Protection. Required advance electronic presentation of cargo information. *Federal Register*, 68(234):68139–68177, 5 July 2003. Final rule.
- [4] DHL. Tracking results detail for 8968906612. Web site, 3 February 2007. <http://track.dhl-usa.com/TrackByNbr.asp?nav=Tracknbr>.
- [5] P. Dutta, M. Grimmer, A. Arora, S. Bibyk, and D. Culler. Design of a wireless sensor network platform for detecting rare, random, and ephemeral events. In *IPSN '05: Proceedings of the 4th international symposium on Information processing in sensor networks*, pages 70–75, Piscataway, NJ, USA, 2005. IEEE Press.
- [6] Erlich Industrial Development Corporation. Resistive humidity sensor board. Web site, 11 January 2006. [http://www.eidusa.com/Interface\\_Boards\\_Humidity\\_Sensors.htm](http://www.eidusa.com/Interface_Boards_Humidity_Sensors.htm).
- [7] M. Feldmeier and J. A. Paradiso. An interactive music environment for large groups with giveaway wireless motion sensors. *Computer Music Journal*, 31(1):50–67, Spring 2007.
- [8] L. Gu and J. A. Stankovic. Radio-triggered wake-up capability for sensor networks. In *10th IEEE Real-Time and Embedded Technology and Applications Symposium (RTAS'04)*, pages 27–36. IEEE Computer Society, May 2004.
- [9] P. Horowitz and W. Hill. *The Art of Electronics*. Cambridge University Press, Cambridge, UK, second edition, 1989.
- [10] S. Jevtic, M. Kotowsky, R. P. Dick, P. A. Dinda, and C. Dowding. Lucid dreaming: Reliable analog event detection for energy-constrained applications. In *Information Processing in Sensor Networks (IPSN/SPOTS) '07*, pages 350–359, 2007.
- [11] X. Jiang, P. Dutta, D. Culler, and I. Stoica. Micro power meter for energy monitoring of wireless sensor networks at scale. In *Information Processing in Sensor Networks (IPSN/SPOTS) '07*, pages 186–195, 2007.
- [12] A. Kambil. RFID: Retail's 800-pound gorilla. *Logistics Today*, 44(10):34–37, Oct. 2003. Supplement.
- [13] Kobitone Audio Company. 25LM025 crystal microphone. Datsheet, 14 July 2005. <http://www.mouser.com/catalog/specsheets/KT-400026.pdf>.
- [14] Linear Technology. LTC1540: Nanopower comparator with reference. Datasheet, 7 December 2004. <http://www.linear.com/pc/downloadDocument.do?navId=H0,C1,C1154,C1004,C1139,P1593,D1777>.
- [15] H. Liu, A. Chandra, and J. Srivastava. eSENSE: Energy efficient stochastic sensing framework for wireless sensor platforms. In *Information Processing in Sensor Networks*.

- works (IPSN/SPOTS) '06*, pages 235–242, Nashville, Tenn., 19–21 April 2006.
- [16] H. Ma and J. A. Paradiso. The FindIT Flashlight: Responsive tagging based on optically triggered micro-processor wakeup. In *UBICOMP 2002*, pages 160–167, Berlin, 2002. Springer Verlag.
- [17] M. Malinowski. CargoNet: Micropower sensate tags for supply-chain management and security. Master's thesis, MIT, EECS Department & Media Lab, Cambridge, Mass., 2 February 2007.
- [18] Measurement Specialties. Measurement specialties 2006 capabilities. Brochure, 21 April 2006. [http://www.meas-spec.com/myMeas/images/catalog/MEASbro\\_14\\_FINAL2.pdf](http://www.meas-spec.com/myMeas/images/catalog/MEASbro_14_FINAL2.pdf).
- [19] M. Moskwa. Basestation: A hand-held datalogger and wireless communication device for use with cargonet. *Advanced Undergraduate Project (AUP) report, MIT Department of EECS*, February 2007.
- [20] Newark InOne. Web site, January 2007. <http://www.newark.com/jsp/home/homepage.jsp>.
- [21] M. Niedermayer, S. Guttowski, R. Thomasius, D. Polityko, K. Schrank, and H. Reichl. Miniaturization platform for wireless sensor nodes based on 3D-packaging technologies. In *5'th International Conference on Information Processing in Sensor Networks, IPSN '06*, pages 391–398. ACM Press, April 19–21 2006.
- [22] M. Ouwerkerk, F. Pasveer, and N. Engin. Sand: A modular application development platform for miniature wireless sensors. In *Proc. of the International Workshop on Wearable & Implantable Body Sensor Networks (BSN2006)*, pages 166–170. IEEE Computer Society, April 3–5 2006.
- [23] J. Paradiso, L. Pardue, K.-Y. Hsiao, and A. Benbasat. Electromagnetic tagging for electronic music interfaces. *Journal of New Music Research*, 32(4):395–409, December 2003.
- [24] J. A. Paradiso, A. Benbasat, and M. Felmeier. General wireless sensor with low-power wake-up. Meeting notes, 29 November 2003.
- [25] C. Park and P. H. Chou. Eco: Ultra-wearable and expandable wireless sensor platform. In *Proc. of the International Workshop on Wearable & Implantable Body Sensor Networks (BSN2006)*, pages 162–165. IEEE Computer Society, April 3–5 2006.
- [26] M. Philipose, J. R. Smith, B. Jiang, A. Mamishev, S. Roy, and K. Sundara-Rajan. Battery-free wireless identification and sensing. *IEEE Pervasive Computing*, 4(1):37–45, January–March 2005.
- [27] Philips. Pcf8563. Datsheet, 12 March 2004. [www.nxp.com/acrobat\\_download/datasheets/PCF8563-04.pdf](http://www.nxp.com/acrobat_download/datasheets/PCF8563-04.pdf).
- [28] A. Pohl, R. Steindl, and L. Reindl. The 'intelligent tire': Utilizing passive SAW sensors-measurement of tire friction. *IEEE Transactions on Instrumentation and Measurement*, 48(6):1041–1046, 1999.
- [29] D. J. Roveti. Choosing a humidity sensor: A review of three technologies. *Sensors*, 18(7):54–58, 1 July 2001.
- [30] M. Sailor. Water sensor experiment. Technical report, UCSD NanoLab, La Jolla, California, 2003. [chem-faculty.ucsd.edu/sailor/research/sensorexperiments.pdf](http://chem-faculty.ucsd.edu/sailor/research/sensorexperiments.pdf).
- [31] Savi Technology. Savi SensorTag ST-676. Datasheet, 11 June 2006. [http://www.savi.com/products/SensorTag\\_676.pdf](http://www.savi.com/products/SensorTag_676.pdf).
- [32] Sencera Co. Ltd. K25K5A resistance humidity sensor specification. Datsheet, 20 May 2002. <http://www.sensorelement.com/humidity/H25K5A%20spec.pdf>.
- [33] Sensirion. SHT1x/SHT7x humidity and temperature sensor. Datasheet, March 2006. [http://www.sensirion.com/en/pdf/product\\_information/Data\\_Sheet\\_humidity\\_sensor\\_SHT1x\\_SHT7x.E.pdf](http://www.sensirion.com/en/pdf/product_information/Data_Sheet_humidity_sensor_SHT1x_SHT7x.E.pdf).
- [34] Sensitech. Coldstream infrastructure. Datsheet, March 2006. [www.sensitech.com/applications/coldstream\\_ppts/ColdStream\\_Infra\\_DataSheet.pdf](http://www.sensitech.com/applications/coldstream_ppts/ColdStream_Infra_DataSheet.pdf).
- [35] J. R. Smith, A. Sample, P. Powledge, A. Mamishev, and S. Roy. A wirelessly powered platform for sensing and computation. In *UbiComp 2006: Eighth International Conference on Ubiquitous Computing*, pages 495–506, Orange County, Calif., 17–21 September 2006.
- [36] C. Swedberg. DHL expects to launch "sensor tag" service by midyear. *RFID Journal*, 19 January 2007. <http://www.rfidjournal.com/article/articleview/2986/>.
- [37] Texas Instruments. MSP430x13xx, MSP430x14xx mixed signal microcontroller. Datasheet, 3 June 2004. <http://www.ti.com/lit/gpn/msp430f135>.
- [38] Texas Instruments. *MSP430x1xx Family User's Guide (Rev. F)*, 28 February 2006. <http://www.ti.com/litv/pdf/slau049f>.
- [39] P. A. Trunick. Vision and visibility govern global supply chains. *Logistics Today*, 47(7):24–26, July 2006.
- [40] U.S. Customs and Border Protection. Container security initiative: 2006–2011 strategic plan, 29 September 2006. [http://www.cbp.gov/linkhandler/cgov/border\\_security/international\\_activities/csi/csi\\_strategic\\_plan.ctt/csi\\_strategic\\_plan.pdf](http://www.cbp.gov/linkhandler/cgov/border_security/international_activities/csi/csi_strategic_plan.ctt/csi_strategic_plan.pdf).
- [41] D. G. Watters, P. Jayaweera, A. J. Bahr, and D. L. Huestis. Design and performance of wireless sensors for structural health monitoring. In D. O. Thompson and D. E. Chimenti, editors, *AIP Conf. Proc. 615: Quantitative Nondestructive Evaluation*, pages 969–976, May 2002.